Int J Adv Manuf Technol (2016) 86:761–767
DOI 10.1007/s00170-015-8214-8

ORIGINAL ARTICLE

Optimization of magnetic arc oscillation system by using double magnetic pole to TIG narrow gap welding

Qingjie Sun[1,2] · Jianfeng Wang[1,2] · Chunwei Cai[3] · Qian Li[1] · Jicai Feng[1,2]

Received: 6 October 2015 / Accepted: 7 December 2015 / Published online: 23 December 2015
© Springer-Verlag London 2015

Abstract A magnetic arc oscillation system for tungsten inert gas (TIG) narrow gap welding is developed to prevent insufficient sidewall fusion and improve efficiency and quality for thick component welding. The characteristic of the system is that a double magnetic pole is induced by exciting current flowing through the field coil to generate the magnetic field within the welding area. This optimization of double magnetic pole not only enhances magnetic flux density compared with conventional single magnetic pole but also provides reliable melting of the sidewall. In this article, a new experimental method for the determination of the resulting heat input into the workpiece is proposed. Measurements of arc voltage and welding current flowing through the sidewalls are used to validate the redistribution of the arc heat. Furthermore, the difference of linear heat input of the sidewalls caused by current division ratio difference and arc voltage difference was the main reason why the formation characteristics occurred.

Keywords Magnetic arc · Formation characteristics · Narrow gap welding · Arc voltage · Current division ratio

✉ Jianfeng Wang
wjf_hitwh@163.com

[1] State Key Laboratory of Advanced Welding and Joining, Harbin Institute of Technology, Harbin 150001, China

[2] Shandong Provincial Key Laboratory of Special Welding Technology, Harbin Institute of Technology at Weihai, Weihai 264209, China

[3] School of Information and Electrical Engineering, Harbin Institute of Technology at Weihai, Weihai 264209, China

1 Introduction

Narrow gap welding reveals an important technique for increasing productivity in the manufacture field of thick-walled components because of significant cost savings, minor distortion, and high quality [1–3]. However, the difficulty of maintaining enough sidewall penetration bottlenecks the development of the tungsten inert gas (TIG) narrow gap welding due to its low heat input and small molten weld pool. In order to minimize the insufficient fusion in TIG narrow gap welding, the pulse arc welding technology [4], which improves the heat input, and the mechanically tungsten electrode oscillating welding technology [5, 6], which promotes the diffusion of the arc heat, were developed to decrease the tendency of the lack of sidewall penetration. These two systems are effective on the sufficient sidewall penetration in some degree, but the former system requires greater heat input with coarse grain. Additionally, increase of the heat input could not absolutely solve the problem [7]. In the case of the latter, this system can have high efficiency for its mechanical oscillation and deep penetration, but the equipment is relatively complex with high cost, which seems to be a problem.

Therefore, a magnetic field externally is utilized in the welding in order to control the arc altering the original arc path under the action of Lorentz force [8, 9]. The interaction of the magnetic field and the electrons within the arc exerts the force, and this force can deflect the arc and consequently homogenize the heat distribution [10]. In the TIG narrow gap welding, many efforts by Belous et al. [11, 12], Starling et al. [13], and Sun et al. [14] have been made in an attempt to apply Lorentz force to overcome the insufficient sidewall penetration and obtain the satisfying welding joint. However, all of the aforementioned studies adopting single magnetic pole were restricted because the single magnetic pole needs more coil turns and larger exciting current. Furthermore, the excitation devices and process procedure were too complicated to

promote their rapid development in comparison with the size of the welding torch. Thus, the study on the reconstruction of the TIG narrow gap welding using the external magnetic field can yield a great significance [15].

Previous studies have concerned primarily on the effect of the magnetic arc oscillation with double magnetic pole on flat position welding [8, 15–20] but typically neglect the application for the TIG narrow gap welding. Therefore, magnetic arc oscillation with double magnetic pole instead of conventional single magnetic pole is selected and observed by TIG welding in narrow groove in this study. The electromagnetic analysis of single and double magnetic poles is observed comparatively via finite element method (FEM), and the effects of magnetic field on arc image and weld formation are thoroughly investigated. The emphasis is placed on the formation characteristics and its generating mechanism from the point of the heat input.

2 Development of welding head and electromagnet

2.1 Experimental principle

The schematic of magnetic arc oscillation in the present study is shown in Fig. 1. The formation principle of magnetic arc oscillation is that a double field core acts as a magnetic conductor connecting to field coil. It is on both sides of the tungsten electrode and lowers into the narrow groove. The arc is periodically oscillated by Lorentz interaction generated by the moving of welding current through the transversal alternating magnetic field. The width of arc oscillation is primarily dependent upon the welding current, the arc length, and the external magnetic field [16, 21].

2.2 FEM of the electromagnet

FEM simulations of the electromagnet by using the commercial finite element package Ansoft Maxwell were performed for the design of electromagnets and analysis of the difference between single and double magnetic poles applied in TIG narrow gap welding. Figure 2 shows the numerical model of the electromagnet composed of field core, field coil, double magnetic pole, and the TIG narrow gap welding torch.

Figure 3 illustrates the magnetic field lines and distributions of magnetic flux density under conditions of 1000 coil turns and 2.5-A exciting current on the coil for single and double magnetic poles. For the single pole magnetic field (Fig. 3a), the magnetic flux density decreases gradually along the magnetic pole axis direction (denoted by the direction of the red arrow) and the density at the center of the welding area is approximately 3.3 mT. However, under the application of double pole magnetic field, the magnetic flux density is on the symmetry axis of the tungsten electrode axis direction and increased to 6 mT in the welding area, which is enough for arc oscillation, as shown in Fig. 3b. Furthermore, using double magnetic pole also produces more uniform distribution of magnetic field lines than that using conventional single magnetic pole. So it is beneficial for the electromagnet with double magnetic pole to improve magnetic flux density increasing by 81.8 % in the welding area and optimize the structure of weld torch.

3 Results and discussion

3.1 Arc image

A high-speed video camera was applied to monitor the magnitude of magnetic arc oscillation qualitatively. The welding experiments were made in a red copper water-cooled groove with a 10-mm root opening under the following conditions: a

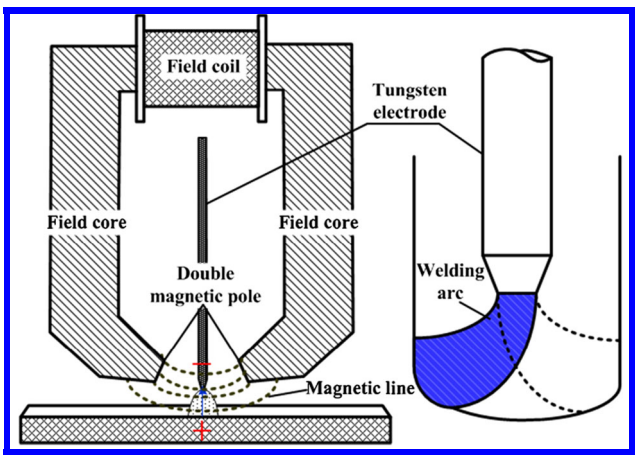

Fig. 1 Schematic of double magnetic pole arc TIG welding

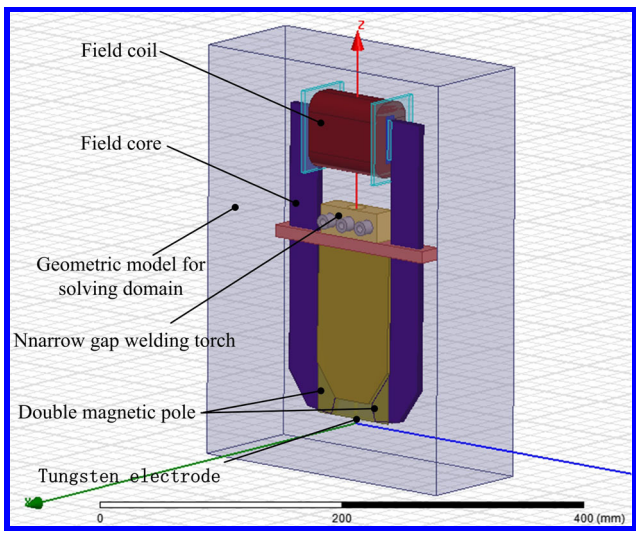

Fig. 2 Finite element method model of the electromagnet with narrow gap welding torch

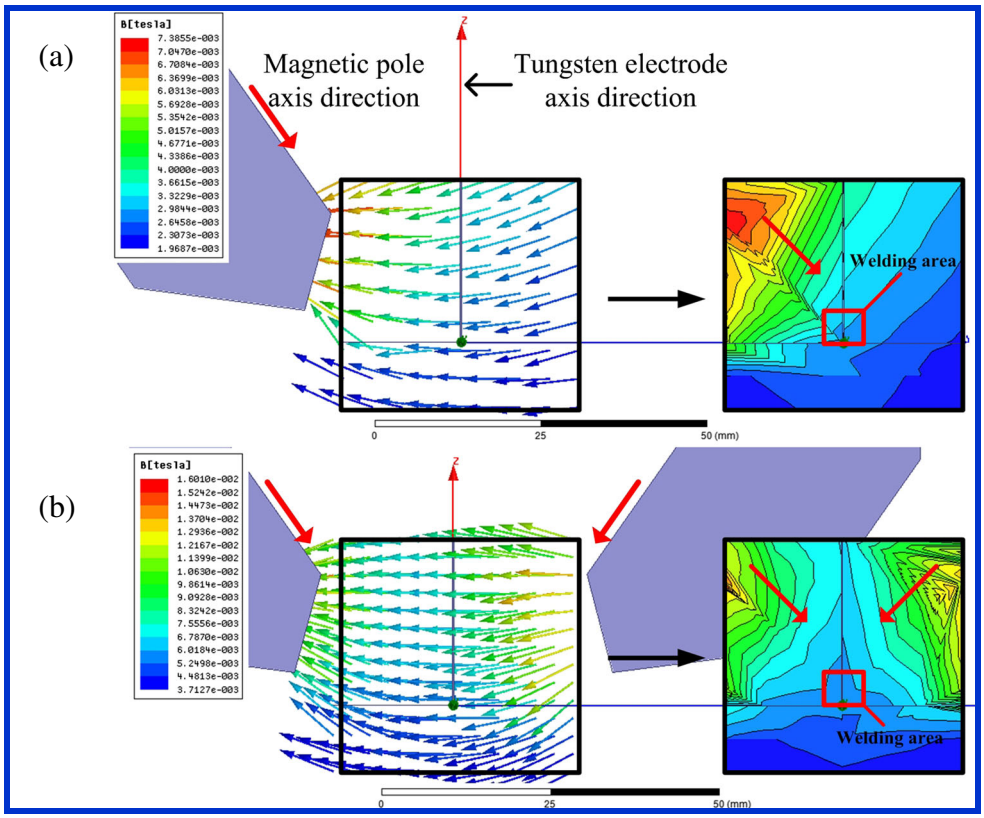

Fig. 3 Magnetic lines and distributions of magnetic flux density under **a** single magnetic pole and **b** double magnetic pole

welding current of 200 A, welding speed of 60 mm/min, contact tip-to-workpiece distance of 3 mm, and magnetic flux density of 6 mT. Table 1 shows the arc images at magnetic field frequency of 5, 10, and 20 Hz, respectively. If arc oscillation width is set to the deviation of the arc centerline [15], then there is no significant change in the oscillation width with increasing magnetic field frequency. Despite operating different frequencies, the arc shape is the same as each other. It merely results in the difference of arc oscillation frequency in one cycle.

Table 1 also displays the arc images with different magnetic flux densities, in which the magnetic field frequency was fixed to 10 Hz. The oscillation width increased with increasing magnetic flux density. When the magnetic flux density was 3 mT, the oscillation width was small, and arc oscillation effect could not be anticipated. At 9 mT, the deflected arc was enlarged and affected near the both sidewalls with high potential to undercut in both sidewalls. When the magnetic flux density was equal to 6 mT, the deflected arc was pointing to the corner between the sidewall and the bottom.

Table 1 Effect of magnetic field frequency and magnetic flux density on arc images

Magnetic field frequency	LEFT	CENTER	RIGHT	Magnetic flux density	LEFT	CENTER	RIGHT
5Hz				3mT			
10Hz				6mT			
20Hz				9mT			

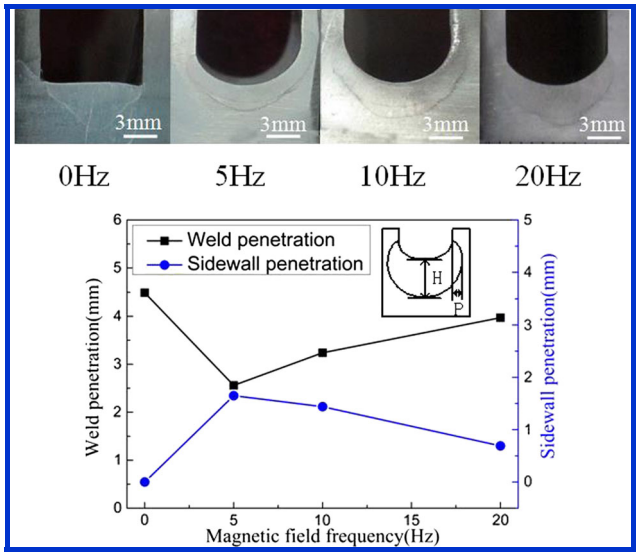

Fig. 4 Effect of magnetic field frequency on bead shape

3.2 Formation of weld bead

Magnetic field frequency and magnetic flux density are the key magnetic field parameters. The study of their effect on the formation of weld bead can promote the understanding of magnetic arc narrow gap welding process. Figure 4 shows the cross sections of weld bead in a magnetic field of 6 mT under various frequencies from 0 to 20 Hz with 304 stainless steel. As 304 stainless steel is a non-magnetic material, applying magnetic field to the welding area cannot lead to flux density loss. As shown, sidewall penetration *P* was virtually zero, while weld penetration *H* was quite large in conventional TIG welding without arc oscillation. It readily resulted in the insufficient fusion into the both sidewalls. While the magnetic field was applied to the arc, it was observed that the side penetration *P* with arc oscillation is deeper than that without oscillation. As

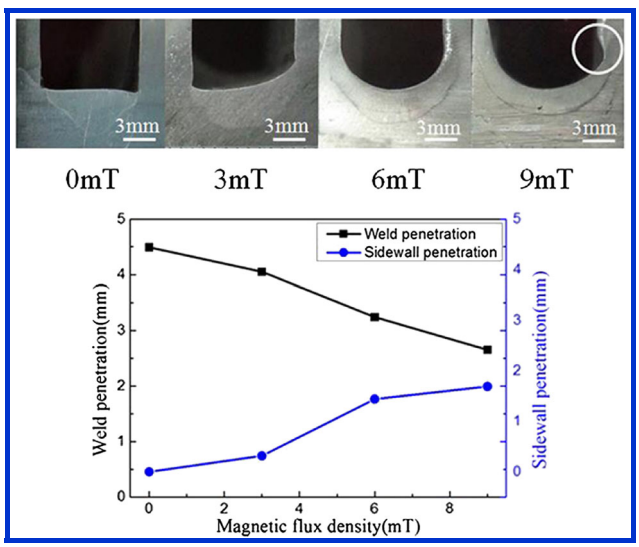

Fig. 5 Effect of magnetic flux density on bead shape

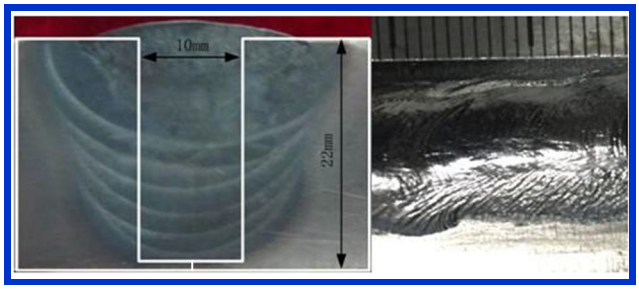

Fig. 6 Cross section of weld joint and weld appearance

the magnetic field frequency varied from 0 to 5 Hz, the side penetration *P* increased obviously to the maximum, while the weld penetration *H* decreased to the minimum. As the magnetic field frequency varied from 5 to 20 Hz, the sidewall penetration *P* apparently decreased and the weld penetration *H* increased with increased magnetic field frequency.

Figure 5 illustrates the cross sections of weld bead with different magnetic flux densities, in which the magnetic flux density varies from 0 to 9 mT and the frequency is fixed at 10 Hz in accordance with previous experiments. Increase of magnetic flux density caused increase of arc oscillation width, as mentioned above. Therefore, sidewall penetration *P* increased with the increase of magnetic flux density. Weld penetration *H* without arc oscillation formed a fingerlike style surface because of the concentration of arc heat. Simultaneously, undercut occurred in the sidewall at a magnetic flux density of 9 mT caused by the excessive oscillation width. Thus, the optimal magnetic flux density should be set to 6 mT for the excellent weld formation without defect. The same results could be achieved by investigating the effect of magnetic flux density on arc images as shown in Table 1.

Based on these observations, the heavy plate TIG narrow gap welding using external magnetic field was carried out. Figure 6 shows the macrophotographs of multilayer single pass welding on 22-mm-thick plate. A deposition of 2–3 mm each layer is obtained at welding current 200 A, arc length 3 mm, welding

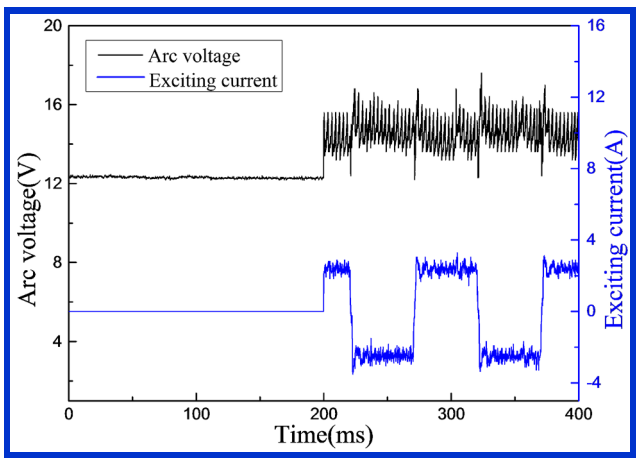

Fig. 7 Welding voltage waveforms of magnetic arc process with AC exciting current of 2.5 A

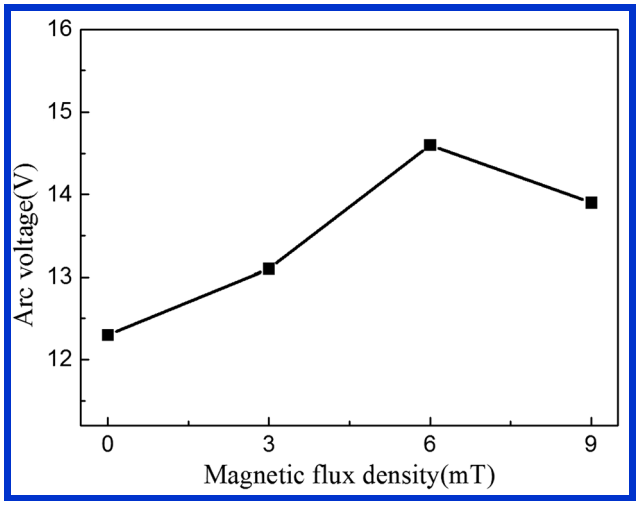

Fig. 8 Effect of magnetic flux density on arc voltage

speed 60 mm/min, wire speed 0.6 m/min, magnetic flux density 6 mT, and magnetic field frequency 10 Hz. The weld formation of each layer is very smooth and shapely without overlap defects or undercut. This demonstrates that using magnetic arc oscillation can share a stable uniform penetration into both sidewalls.

3.3 Formation characteristics

The magnetic arc welding process can effectively improve the weld formation through the above research in TIG narrow gap welding. In other words, magnetic arc welding process presents technical advantages for the redistribution of linear heat input. Accordingly, the effect of magnetic arc welding process on formation characteristics was explored through using the linear heat input in both sidewalls as the entry point in this paper. The linear heat input is dependent on welding current, arc voltage, and welding speed [7, 22]. However, magnetic arc oscillation leads to a change of arc length, which in turn periodically changes arc voltage and welding current flowing through the sidewalls [12, 15]. Hence, the effects of arc voltage and welding current flowing through the sidewalls on the linear heat input can be investigated as follows by using external magnetic field.

The waveforms of arc voltage were monitored by using an oscilloscope to ascertain the relationship between arc voltage and exciting current, as shown in Fig. 7. It implies that arc voltage is seriously affected by magnetic field in the welding area. Subsequently, assuming root-mean-square (RMS) value of the arc voltage in an arc oscillation period as a valid value, the relationship between arc voltage and magnetic flux density is shown in Fig. 8. It can be seen that arc voltage has a peak at magnetic flux density of 6 mT. With further increase of magnetic flux density, the arc voltage presents a decreased trend. The reason of this behavior can be explained as follows.

The schematic diagram of the variation of effective arc length is shown in Fig. 9. When arc was deflected to the extreme position where the value of S_b was larger than that of S_s (Fig. 9a), the value of effective arc length L was larger than that of contact tip-to-workpiece distance. Therefore, the arc voltage increased obviously with an increase in magnetic flux density. At 6 mT, the largest arc voltage was occurred to where S_b was equal to S_s (Fig. 9b), and the effective arc length L was the maximum value. It means that the deflected arc was shifted to the intersection of the sidewall and bottom. When magnetic field was over 6 mT where S_b was smaller than S_s (Fig. 9c), the effective arc length L was inferior to the maximum value. Therefore, the arc voltage decreased gradually.

Figure 10 shows the experimental scheme of the unit to measure welding current quantificationally. In order to measure the current flowing through the bottom I_b and sidewall I_s, respectively, a split-anode method of Nestor [23] is applied to determine the distribution of the welding current. The narrow groove is reproduced via two decoupled copper blocks, and the border of two decoupled copper blocks is isolated with 0.1-mm-thick insulating board, as shown in Fig. 10a. The variation of I_b and I_s with the change of arc oscillation time is shown in Fig. 10b. The magnitude of arc oscillation can be characterized clearly by welding current division ratio δ:

$$\delta = \frac{I_s}{I_w} \tag{1}$$

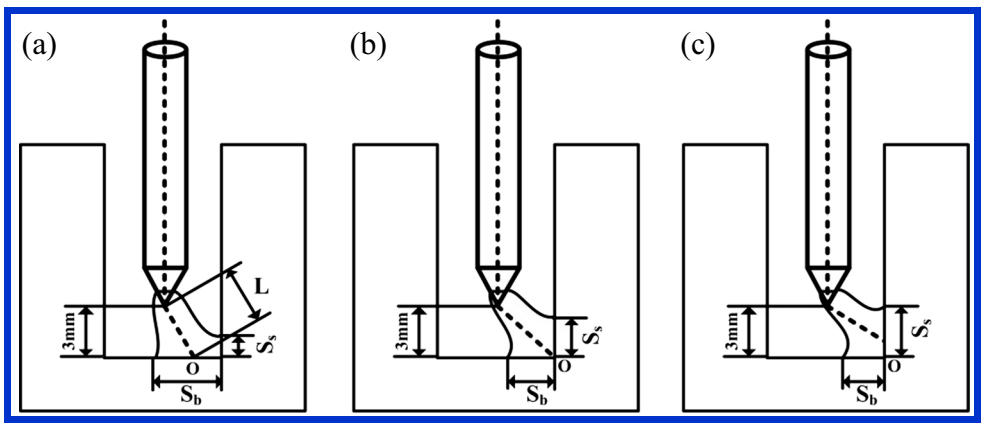

Fig. 9 Schematic of effective arc length when the arc is deflected to the extreme position: (**a**) $S_b > S_c$; (**b**) $S_b = S_c$; (**c**) $S_b < S_c$

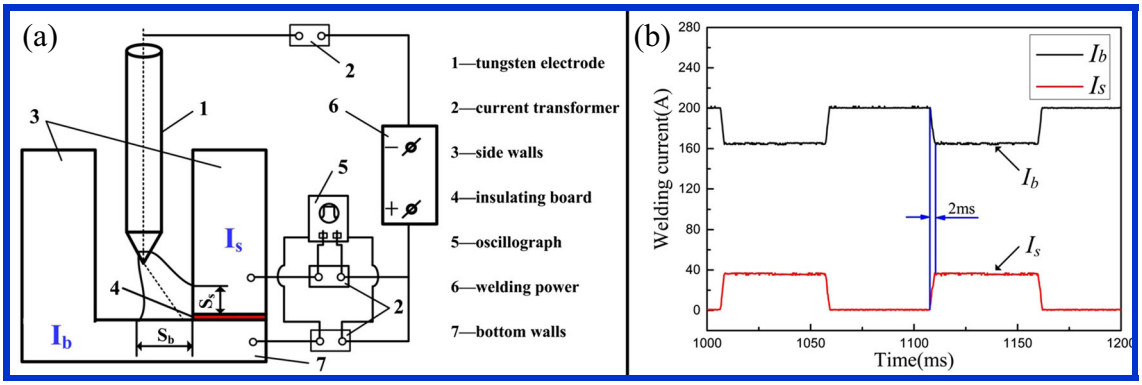

Fig. 10 The scheme of the unit to measure the welding current: **a** schematic diagram of the unit to measure the current; **b** the current flowing through the sidewall at the right side I_s and the bottom I_b

where I_s is the current flowing through the sidewall at the right side, and I_w is the total welding current.

The value of δ is nearly proportional to magnetic flux density, as shown in Fig. 11. At 6 mT, the fraction of current flowing through the sidewall is 51.9 % of the total welding current, which exactly coincides with the largest arc voltage. So the variation of current flowing through the sidewall shows a fairly good agreement with that of arc voltage due to arc oscillation.

Based on these observations, the total linear heat input E_w is evaluated as

$$E_w = \frac{UI_w}{V_w} \tag{2}$$

where V_w is the welding speed, I_w is the total welding current, and U is the arc voltage.

When the welding speed V_w and total welding current I_w were determined, the relationship between arc voltage U and the total linear heat input E_w could be obtained combining the arc voltage U shown in Fig. 8. The calculated result of E_w in various magnetic flux densities is shown in Fig. 12. The value of E_w is directly proportional to the value of U, while it is irrelevant to magnetic field parameters.

In particular, the change of the current flowing through both sidewalls can be attributed to the redistribution of the linear heat input in both sidewalls of E_s. The effect of welding current flowing through both sidewalls on E_s was implemented to estimate the formation characteristics. So the linear heat input in both sidewalls can be calculated as

$$E_s = \eta \frac{UI_w\delta}{V_w} \tag{3}$$

The coefficient η is induced by considering the factor that when arc was deflected from one sidewall to the other, the welding current is not instantaneously changed but with a 2-ms lag as shown in Fig. 10b, which can cause that the portion of arc heat in both sidewalls may be transferred to the bottom under the action of periodical arc deflection compared to the unidirectional magnetic field. Increase of magnetic field frequency causes increase of arc oscillation frequency, which may transfer the heat input to the bottom and increase the heat

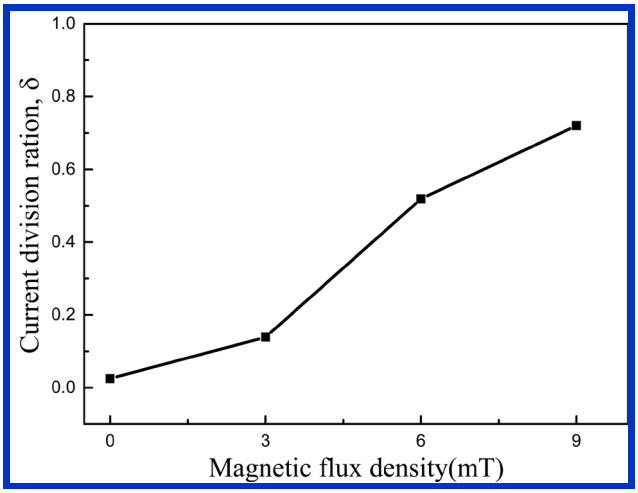

Fig. 11 Dependence of the fraction of the current in a sidewall on the magnetic flux density

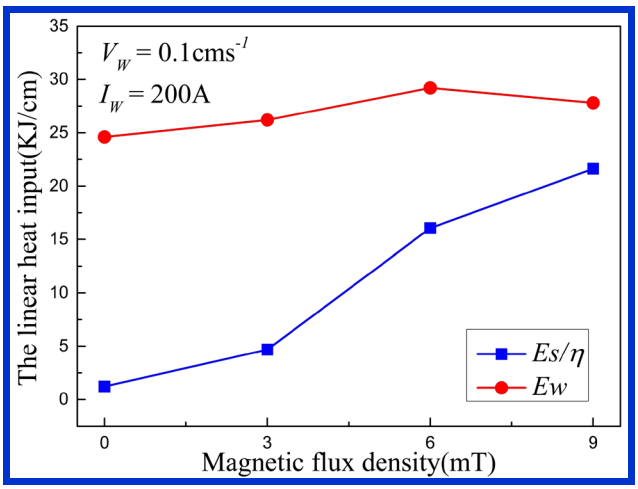

Fig. 12 The value of E_w and E_s/η in different magnetic flux densities

input in the bottom in return and, consequently, the value of η decreases gradually.

Figure 12 also shows the value of E_s/η in different magnetic flux densities. If magnetic field frequency remains unchanged, then value of η represents a constant component. The difference of the two linear heat inputs ($E_w - E_s$) represents the linear heat input of the bottom and reaches the maximum when there is no magnetic field. It decreases with increasing magnetic flux density, meaning that the effective heat input decreases in the bottom and increases in the sidewalls. This is the reason that joint characteristics generate owing to the influence of magnetic flux density as shown in Fig. 5.

If magnetic field frequency changes, then value of η represents a variable component. The value of η is decreased with increasing magnetic field frequency, which subsequently leads to a decrease of E_s. It means the decrease of the effective heat input in the sidewalls and increase in the bottom with increasing magnetic field frequency, which exactly coincides with Fig. 4. Therefore, energy distribution characteristics affected by magnetic arc process will be favorable for sidewall penetration in narrow gap welding.

4 Conclusions

1. A magnetic arc system generated by the double magnetic pole for TIG narrow gap welding was employed. As compared to the traditional type, this new system was made smaller and lighter, and the magnetic flux density can enhance by 81.8 %.
2. The increase of magnetic flux density applied in the welding area caused the increase of arc oscillation width. The sidewall penetration increased obviously with increased magnetic flux density or decreased magnetic field frequency.
3. Magnetic arc oscillation resulted in the change of arc voltage and welding current flowing through both sidewalls, which in turn caused the redistribution of arc heat. The welding current division ratio is nearly proportional to magnetic flux density, and arc voltage has the peak at magnetic flux density of 6 mT.

Acknowledgement We are grateful to the National Natural Science Foundation of China (Grant No. 51475104, 51435004) and the State Key Development Program for Basic Research of China (Grant No. 2013CB035500) for the financial support to this study.

References

1. Wang JY, Ren YS, Yang F, Guo HB (2007) Novel rotation arc system for narrow gap MAG welding. Sci Technol Weld Join 12(6):505–507
2. Li W, Gao K, Wu J, Hu T, Wang J (2014) SVM-based information fusion for weld deviation extraction and weld groove state identification in rotating arc narrow gap MAG welding. Int J Adv Manuf Technol 74(9-12):1355–1364
3. Xu WH, Lin SB, Fan CL, Yang CL (2014) Evaluation on microstructure and mechanical properties of high-strength low-alloy steel joints with oscillating arc narrow gap GMA welding. Int J Adv Manuf Technol 75(9-12):1439–1446
4. Matsuda F (1984) Narrow gap welding. Japan Welding Society/ Kuroki Press, Osaka
5. Turner PW, Eichenberger GD (1982) Fitup tolerances for mechanized gas tungsten arc welding large-diameter Pipe. Weld J 61(9): 283–292
6. Shtrikman MM, Pavlov AS (1983) Determining the optimum penetration depth in welding in a slit-like gap with transverse oscillations of the arc. Weld Prod 30(3):38–41
7. Yang CL, Guo N, Lin SB, Fan CL, Zhang YQ (2009) Application of rotating arc system to horizontal narrow gap welding. Sci Technol Weld Join 14(2):172–177
8. Shoichi M, Yukio M, Koki T, Yasushi T, Yukinori M, Yusuke M (2013) Study on the application for electromagnetic controlled molten pool welding process in overhead and flat position welding. Sci Technol Weld Join 18(1):38–44
9. Liu YB, Sun QJ, Liu JP, Wang SJ, Feng JC (2015) Effect of axial external magnetic field on cold metal transfer welds of aluminum alloy and stainless steel. Mater Lett 152:29–31
10. Bouabdallah S, Bessaïh R (2012) Effect of magnetic field on 3D flow and heat transfer during solidification from a melt. Int J Heat Fluid Fl 37:154–166
11. Belous VY, Akhonin SV (2007) Influence of controlling magnetic field parameters on weld formation in narrow-gap argon-arc welding of titanium alloys. Paton Weld J 59(4):2–5
12. Belous VY (2011) Conditions for formation of defect-free welds in narrow-gap magnetically controlled arc welding of low titanium alloys. Paton Weld J 3:16–18
13. Starling CMD, Marques PV, Modenesi PJ (1995) Statistical modelling of narrow-gap GTA welding with magnetic arc oscillation. J Mater Process Tech 51(1):37–49
14. Sun QJ, Hun HF, Li WJ, Liang YC (2013) Electrode tips geometry and penetrating in narrow gap welding. Sci Technol Weld Join 18(3):198–203
15. Kang YH, Na SJ (2003) Characteristics of welding and arc signal in narrow groove gas metal arc welding using electromagnetic arc oscillation. Weld J 82(5):93–99
16. Ecer GM (1980) Magnetic deflection of the pulsed current welding arc. Weld J 59(6):99–107
17. Chang YL, Liu XL, Lu L, Babkin AS, Lee YB, Gao F (2014) Impacts of external longitudinal magnetic field on arc plasma and droplet during short-circuit GMAW. Int J Adv Manuf Technol 70(9-12):1543–1553
18. Bachmann M, Avilov V, Gumenyuk A, Rethmeier M (2013) About the influence of a steady magnetic field on weld pool dynamics in partial penetration high power laser beam welding of thick aluminium parts. Int J Heat Mass Tran 60:309–321
19. Zhong QL, Yong BL, Ya SW, Chen GL (2005) Numerical analysis of a moving gas tungsten arc weld pool with an external longitudinal magnetic field applied. Int J Adv Manuf Technol 27(3-4):288–295
20. Kang YH, Na SJ (2002) A study on the modeling of magnetic arc deflection and dynamic analysis of arc sensor. Weld J 81(1):8–13
21. Sundaresan S, Ram GDJ (1999) Use of magnetic arc oscillation for grain refinement of gas tungsten arc welds in α–β titanium alloys. Sci Technol Weld Join 4(3):151–160
22. Su YC, Hua XM, Wu YX (2014) Influence of alloy elements on microstructure and mechanical property of aluminum–steel lap joint made by gas metal arc welding. J Mater Process Tech 214(4):750–755
23. Nestor OH (1962) Heat intensity and current density distributions at the anode of high current, inert gas arcs. J Appl Phys 33(5):1638–1648